THE ASTROPHYSICAL JOURNAL, 442:589–596, 1995 April 1

MULTIFREQUENCY OBSERVATIONS OF KAZ 102 DURING THE *ROSAT* ALL-SKY SURVEY

A. TREVES,[1] H. H. FINK,[2] M. MALKAN,[3] S. J. WAGNER,[4] B. J. WILKES,[5] F. BAGANOFF,[3] J. HEIDT,[4] E. PIAN,[1] A. SADUN,[6] S. SCHAEIDT,[2] J. T. BONNELL,[7] W. BRINKMANN,[2] D. DE MARTINO,[8] L. MARASCHI,[9] E. G. TANZI,[10] M. H. ULRICH,[11] AND W. WAMSTEKER[8]

Received 1994 June 13; accepted 1994 October 10

ABSTRACT

The bright quasar Kaz 102, which lies in the vicinity of the North Ecliptic Pole, was monitored during the *ROSAT* All Sky Survey for 121.5 days from 1990 July 30 to 1991 January 25. In the course of the survey, optical photometry with various filters was performed at several epochs, together with UV (*IUE*) and optical spectrophotometry. The spectral energy distribution in the 3×10^{14}–3×10^{17} Hz range is obtained simultaneously among the various frequencies to $\lesssim 1$ day. No clear case of variability can be made in the X-rays, while in the optical and UV variability of 10%–20% is apparent. An analysis of *IUE* and *Einstein* archives indicates a doubling timescale of years for the UV and soft X-ray flux. The X-ray photon index, which in 1979 was rather flat ($\Gamma = 0.8^{+0.6}_{-0.4}$), in 1990/1991 was found to be $\Gamma = 2.22 \pm 0.13$, a typical value for radio-quiet quasars in this energy range. The overall energy distribution and the variability are discussed.

Subject headings: galaxies: active — quasars: individual (Kaz 102) — ultraviolet: galaxies — X-rays: galaxies

1. INTRODUCTION

During the six month survey phase *ROSAT* observed the north and south ecliptic poles once per orbit with the PSPC experiment. The regions in the vicinity of the poles were therefore monitored for a duration unprecedented for X-ray telescopes. Because of this unique opportunity, multifrequency observations of active galactic nuclei in the polar region were organized, with the aim of studying correlated variability (see, e.g. Brinkmann & Trümper 1992).

In this paper, we examine the close-by, radio-quiet quasar Kaz 102 ($m_B \simeq 16$, $z = 0.136$), which is a strong X-ray source and has the hardest spectrum of any quasar observed with the *Einstein Observatory* (Wilkes & Elvis 1987). Preliminary results were reported by Treves et al. (1992), and by Walter & Fink (1993).

The paper is structured as follows: in § 2 the *ROSAT* X-ray light curve and spectrum are presented and compared with *Einstein* observations. Optical light curves and optical and UV spectrophotometry are described in § 3. The results are discussed in § 4.

[1] Scuola Internazionale Superiore di Studi Avanzati, Via Beirut 2-4, 34014 Trieste, Italy.
[2] Max Planck-Institute für Extraterrestriche Physik, Giessenbachstrasse, 85740 Garching bei München, Germany.
[3] University of California, Los Angeles, CA 90024-1562.
[4] Landessternwarte Heidelberg-Königstuhl, Königstuhl, 69117 Heidelberg, Germany.
[5] Harvard-Smithsonian Center for Astrophysics, 60 Garden Street, Cambridge, MA 02138.
[6] Department of Physics and Astronomy, Agnes Scott College, 141 East College Avenue, Decatur, GA 30030.
[7] Goddard Space Flight Center, Greenbelt, MD 20771.
[8] ESA, *IUE Observatory*, P.O. Box 50727, 28080 Madrid, Spain.
[9] Dip. di Fisica, Università de Genova, Via Dodecaneso 33, 16133 Genova, Italy.
[10] Istituto di Fisica Cosmica, Consiglio Nazionale delle Ricerche, Via Bassini 15, 20133 Milano, Italy.
[11] European Southern Observatory, Karl-Schwarzschild-Strasse 2, 85748 Garching bei München, Germany.

2. X-RAY OBSERVATIONS

2.1. *Light Curve*

The source, which lies at $\sim 1°$ from the north ecliptic pole, was observed by *ROSAT* during the survey phase for 121.5 days, in two parts: (1) from 1990 July 30 to October 31 and (2) from 1990 December 27 to 1991 January 25. Each exposure had a typical effective (i.e., on-axis) duration of 10–30 s, and the separation between the exposures was the satellite orbital period of 96 minutes. A special procedure was used for the extraction of survey data. The source + background counts were estimated from a 300″ radius circle centered on the X-ray source position with the background taken from a 610″ radius circle separated from the source by 17′. The net raw source + background counts were ~ 6100, with an estimated background contribution of 1600 counts. The effective exposure time was $\sim 24{,}000$ s. Taking into account vignetting corrections derived from energy dependent flat-field exposures of the detector's field of view (Snowden et al. 1994) this yields an average source count rate of ~ 0.3 counts s^{-1} superposed on a background of ~ 0.1 counts s^{-1}. While the source was marginally observable during each orbit, integrations over a day or more are required in order to reduce the statistical error. Figure 1*a* gives the light curve with a two-day integration. Only statistical errors are reported. The reduced χ^2 under the hypothesis of constancy is 1.3, with a formal probability of constancy of 4.6%. However, systematic study of light curves of a complete survey sample shows that variability should not be considered as reliable for $\chi^2 \lesssim 2$ (Schaeidt 1994). Therefore we conclude that no solid case for variability can be made. We note the appearance of possible dips at MJD = 8125 and at MJD = 8160 (Figure 1*a*).

2.2. *X-Ray Spectrum*

A standard minimization procedure was used to fit the background corrected spectrum, from the cumulative exposure, to the following models: (1) a single power-law model with absorption taken as a free parameter; and (2) a power law plus a blackbody model with absorption fixed at the Galactic value

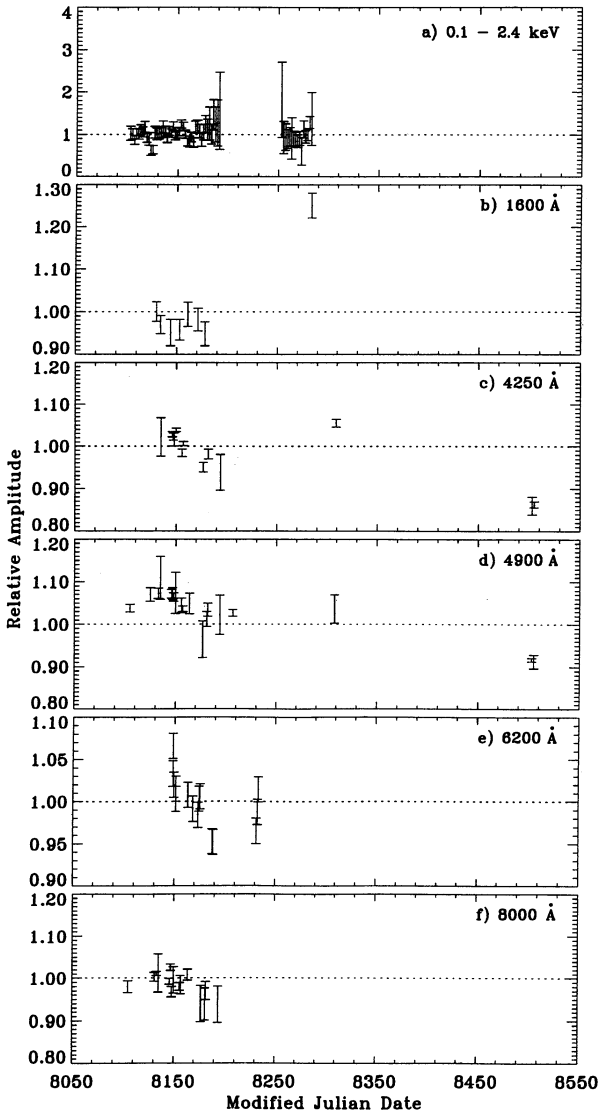

FIG. 1.—Light curves of Kaz 102 normalized to the average (see Table 5): (*a*) X-ray counts s^{-1}; the data are binned with a 2 day flux integration; (*b*) UV; (*c*) *B* band (from Lick observations); (*d*) *g* band (from Lick observations); (*e*) *R* band (from Heidelberg observations); (*f*) *I* band (from Lick observations).

[$N_H = (5.0 \pm 0.3) \times 10^{20}$ cm^{-2}, Elvis, Lockman, & Wilkes 1989]. Details are given in Table 1 and Figure 2. The entire *ROSAT* sensitivity range (0.1–2.4 keV) was considered. We verified that the power-law fit remains unchanged within the errors excluding the channels below 0.2 keV, which, in the opinion of some authors, may be affected by instrumental uncertainties. The results of the analysis are consistent with those reported by Treves et al. (1992) and Walter & Fink (1993), which were based on the analysis of a fraction of the data examined here, using a preliminary form of the response matrices. Note that the hydrogen column density given by fit (*a*), $N_H = (4.08 \pm 0.53) \times 10^{20}$ cm^{-2}, is somewhat lower than the Galactic one.

The source was observed with the *Einstein Observatory* back in 1979 June and the spectrum was discussed in Wilkes & Elvis (1987). Here we are presenting a new analysis of the spectrum based on somewhat improved calibration matrices. A total of ~600 source photons were detected. A best fit was searched for

TABLE 1

PARAMETERS OF THE *ROSAT* SPECTRUM[a]

Parameter	Power Law[b]	Power Law + Blackbody[c]
A_{pl}[d]	2.71 ± 0.28[e]	2.65
A_{bb}[f]	...	0.58
Γ	2.22 ± 0.13	2.29 ± 0.12
N_H[g]	4.08 ± 0.53	5.0
kT[h]	...	21 ± 15
χ^2/d.o.f.	0.879	0.843

[a] The spectrum is deabsorbed after Morrison & McCammon 1983.

[b] $f_{pl}(E, A_{pl}, \Gamma, E_0)dE = A_{pl}(E/E_0)^{-\Gamma}dE$; $E_0 = 2$ keV.

[c] $f_{pl} + f_{bb}$, with $f_{bb}(E, A_{bb}, T)dE = [A_{bb}(E/kT)^2]/[kT(e^{E/kT} - 1)]dE$.

[d] In 10^{-4} photons s^{-1} cm^{-2} keV^{-1}.

[e] The quoted errors represent 1 σ uncertainties on the fitted parameters.

[f] In photons s^{-1} cm^{-2}.

[g] Equivalent hydrogen column density in 10^{20} cm^{-2}. For the pl + bb fit, N_H is fixed at the Galactic value.

[h] In electron volts.

with an absorbed power-law fit. We obtain $N_H = (1.1^{+7.8}_{-1.0}) \times 10^{20}$ cm^{-2}, $\Gamma = 0.8^{+0.6}_{-0.4}$ and $F_{1\,keV} = 0.34$ μJy ($\chi^2 = 0.69$). These parameters are consistent with the previous analysis of Wilkes & Elvis (1987).

Comparing the *Einstein* flux with the average 1990/1991 flux from our *ROSAT* observations ($F_{1\,keV} = 0.85$ μJy), an increase at 1 keV of more than a factor of 2 is apparent. The energy index/N_H plots of the two observations, which are shown in Figure 3, indicate on the one hand the much reduced uncertainty of the *ROSAT* spectrum due to higher photon statistics and to superior resolution of the detector. On the other hand, a spectral variation of the source is strongly suggested, as from the fact that the plots are completely disjoint. As apparent from the figure, in the *Einstein* observation the column density is poorly constrained. Fixing its value at $N_H = 4.1 \times 10^{20}$ cm^{-2}, the spectral indices for *ROSAT* and *Einstein* are, respectively, $\Gamma_R = 2.20 \pm 0.06$ and $\Gamma_E = 1.1 \pm 0.2$ (1 σ), yielding $\Delta\Gamma = 1.10 \pm 0.21$. The variation in the spectral index therefore appears significant at the 5 σ level.

TABLE 2

OPTICAL AND UV SPECTROPHOTOMETRY

Instrument	Date	Exposure Time[a]
Ground-based Observations		
Lick	1990 Aug 01	20
Lick	1990 Aug 31	10
Lick	1990 Sep 15	10
Lick	1990 Sep 29	13
MMT	1990 Oct 14	20
Lick	1991 Feb 21	10
IUE Observations		
SWP 31032	1987 May 23	395
LWP 10810	1987 May 22	385
SWP 39545	1990 Aug 27	435
SWP 39558	1990 Aug 31	388
SWP 39608	1990 Sep 10	428
SWP 39664	1990 Sep 19	420
SWP 39718	1990 Sep 27	423
SWP 39788	1990 Oct 07	379
SWP 39831	1990 Oct 14	405
LWP 19011	1990 Oct 14	390
SWP 40961	1991 Jan 27	333

[a] In minutes.

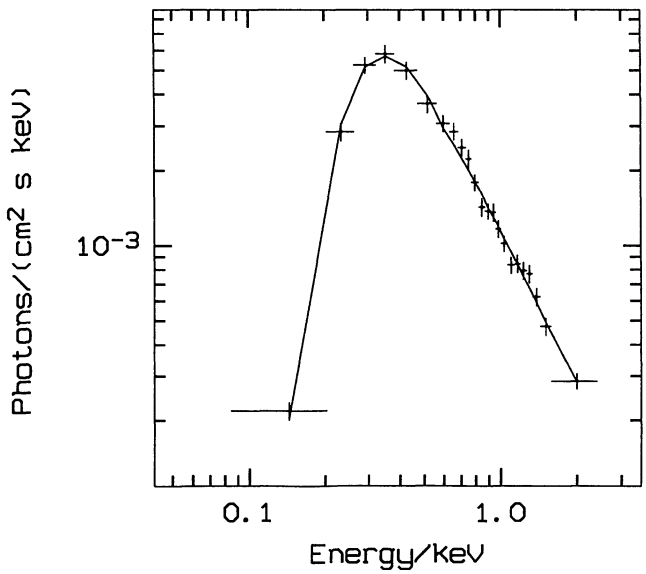

FIG. 2a

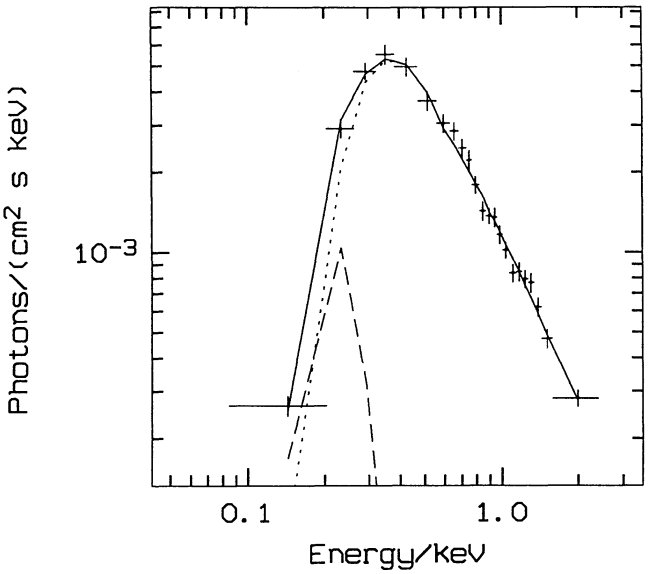

FIG. 2b

FIG. 2.—*ROSAT* average spectrum: (*a*) power-law fit plus absorption; (*b*) power law plus blackbody fit with absorption fixed to the Galactic value. The dashed line represents the blackbody curve decomposed from the power law.

3. OPTICAL-UV OBSERVATIONS

3.1. *Spectroscopy*

Optical spectrophotometry of the source was performed at the Multiple Mirror Telescope (MMT) and at the Lick 3 m telescope (see Table 2, top section and Fig. 4).

The MMT spectrum was obtained using the blue spectrograph with a wavelength range 3200–6400 Å and a resolution of 5 Å (1″ × 3″ aperture, 300 grooves per millimeter grating). Conditions were photometric and the spectrum was calibrated by taking a spectrum of both the quasar and a nearby flux standard star through a 5″ diameter circular aperture. The small-aperture spectrum was then normalized to the continuum shape and level of the flux calibrated, large-aperture spectrum. We estimate the photometric errors to be ~10%.

The MMT spectrum can be directly compared with a spectrum of the source taken in April of 1988 with the Faint Object Grism Spectrograph (FOGS) on the MMT (Shastri et al. 1993).

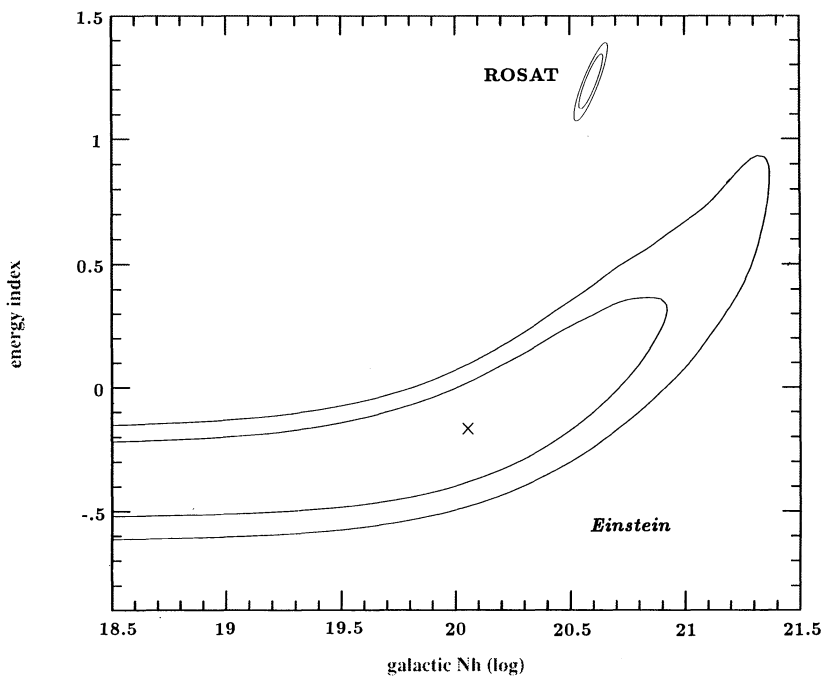

FIG. 3.—Energy index/N_H fit contour of the *Einstein* spectrum compared with the one from *ROSAT*. The two curves of each contour represent the 1 and 1.5 σ confidence levels.

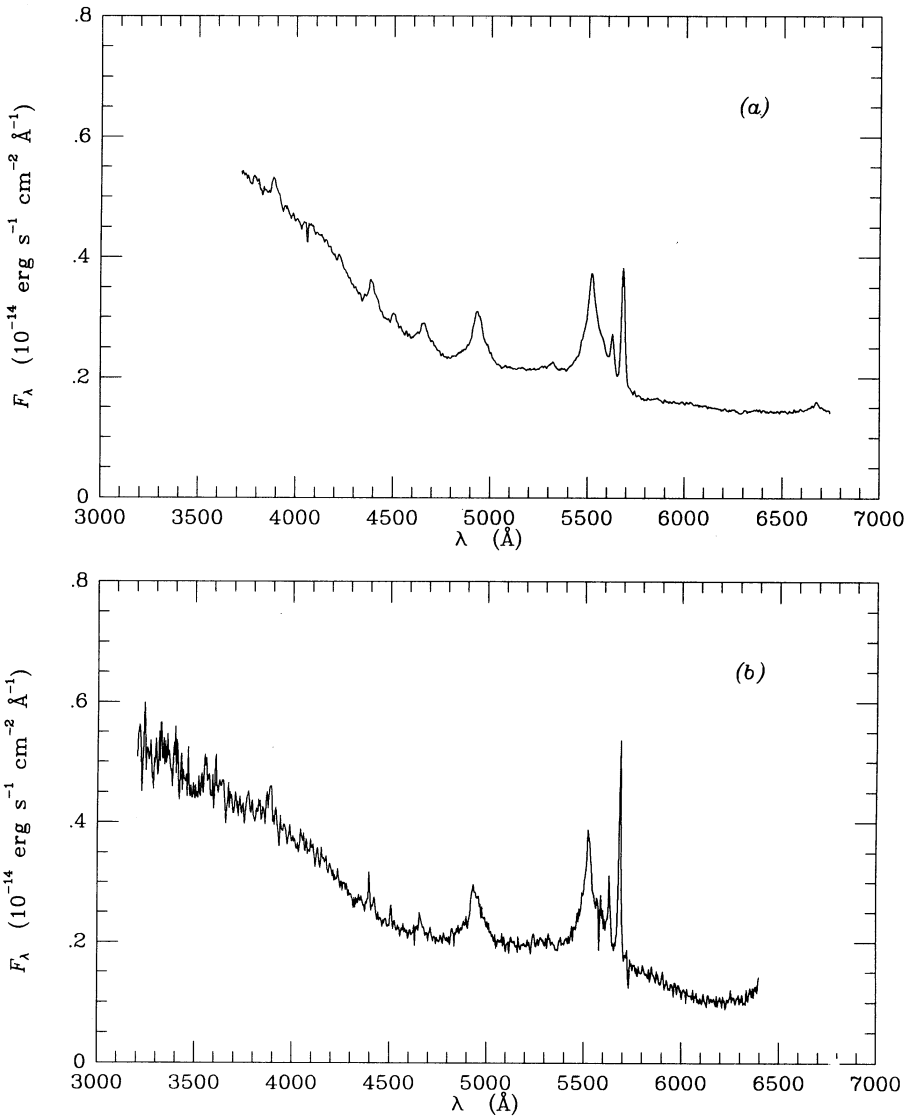

FIG. 4.—Optical spectrophotometry (see Table 2): (*a*) average of the five spectra from the Lick Observatory; (*b*) MMT spectrum

A comparison of the continuum level shows an increase of ~10% in 2.5 yr. Given the estimated errors of ~10%, this change is not significant. Note that in Shastri et al. the ordinate scale of the spectrum should be corrected upward by a factor of 5.

Five spectra of Kaz 102 were obtained with the Lick Observatory 3 m telescope using the UV/Schmidt Camera with a 5″ slit. This instrument uses an 800 × 800 pixel TI CCD which is UV flooded before cool down for enhanced sensitivity at blue wavelengths. A 300 l mm^{-1} grating was used to cover the wavelength range from 3600 to 6600 Å with a spectral resolution of 4 Å pixel^{-1}. Standard star observations were made prior to and after observations of Kaz 102. Between 3 and 7 spectrophotometric standard stars were observed during the course of each night. Good agreement between gain curves through out a night indicated that the August and September nights in 1990 were photometric. Only 1991 February 21 revealed the effects of variable cloud cover and seeing. For the August and September nights, the errors on spectrophotometry are estimated to be 5%–10%.

The MMT spectrum is similar to the average one taken at the Lick Observatory, with an average discrepancy of 13.5% and a more marked percentage difference at shorter wavelengths, probably due to higher variability of the source at higher frequencies and to the nonsimultaneity of MMT and Lick spectrophotometry.

Nine *IUE* spectra were gathered for this project with the SWP (1200–1950 Å) and the LWP (2000–3000 Å) cameras. For comparison, we have also retrieved two archival spectra from 1987 (see also Elvis et al. 1994). Details are given in Table 2, lower panel, and in Figure 5. The spectra were analyzed using an adaptation of the Gaussian Extraction Procedure (Urry & Reichert 1988) to the MIDAS package and calibrated after Bohlin et al. (1990; SWP) and Cassatella, Lloyd, & Gonzalez-Riestra (1988; LWP). The UV fluxes were integrated over the band 1450–1700 Å, with uncertainties evaluated as in Falomo et al. (1993). Notice that in 3 years the source has brightened by ~40% (Fig. 5).

Strong emission lines are apparent in both the optical (Hγ, Hβ, and [O III]) and UV (Lyα, Si IV, C IV, C III]) spectra (see

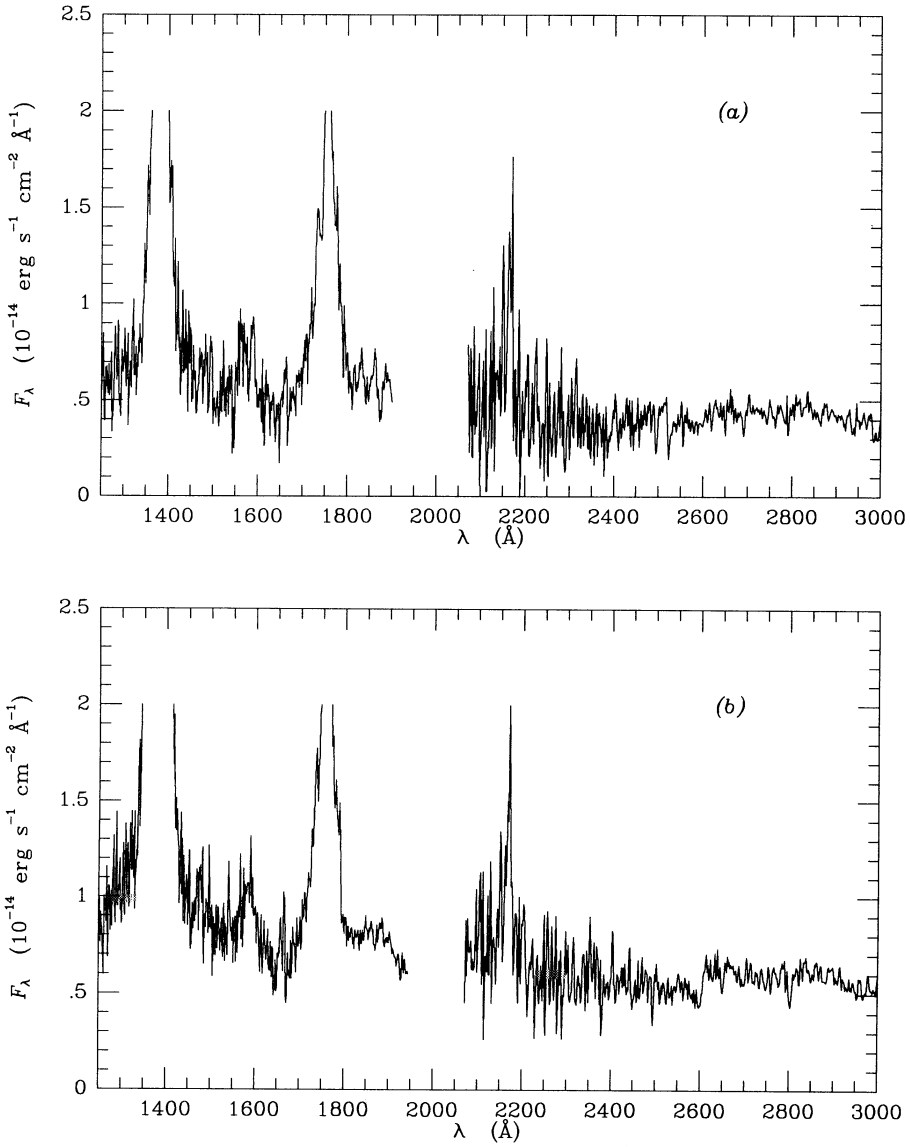

FIG. 5.—*IUE* spectra: (*a*) 1987 May 22–23 (SWP 31032 and LWP 10810); (*b*) 1990 October 14 (SWP 39831 and LWP 19011). The Lyα and C IV emission lines are truncated.

Table 3 and Figs 4 and 5). The intensities and equivalent widths are evaluated with errors of 10%–20%, mainly due to the uncertainty in the estimate of the underlying continuum. The intensity ratios are typical for quasars (see, e.g., Netzer 1990).

3.2. *Photometry*

Optical photometry was performed in various broadband filters at the Lick Observatory, Capilla Peak Observatory (New Mexico), and at the Heidelberg Landessternwarte (Tables 4 and 5).

Twenty-three nights of direct imaging were done on the Lick Observatory 1 m Nickel telescope using a 500 × 500 pixel CCD. Eighteen of these nights were either photometric or very nearly so. The field of view was 4.′5 on a side and the plate scale was ~0.″6 pixel^{-1}. High-precision (2%–3%) relative photometry was obtained by using nine comparison stars to adjust all frames to a common flux level. Observations were made with Johnson *B*, Gunn *g*, and Kron-Cousins *I* filters. An additional 10 nights of direct imaging were obtained on the Lick 3

TABLE 3

UV AND OPTICAL EMISSION LINES

Ion	I^a	EW^b
Lyα λ1216.....	220	210
Si IV λ1403.....	19	26
C IV λ1549.....	86	100
C III] λ1909.....	13	17
Hγ λ4340.....	9	42
Hβ λ4861.....	17	90
[O III] λ5007.....	5	29

[a] Observed line intensity in 10^{-14} ergs s^{-1} cm^{-2}.

[b] Observed line equivalent width in angstroms.

TABLE 4

OPTICAL PHOTOMETRY

Date	*B*	*g*	*V*	*R*	*I*
		Lick Observatory			
1990 Aug 01	...	15.688 ± 0.010	...	...	15.385 ± 0.017
1990 Aug 21	...	15.655 ± 0.018	...	...	...
1990 Aug 27	...	...	...	...	15.359 ± 0.012
1990 Aug 29	...	15.652 ± 0.013	...	...	15.351 ± 0.006
1990 Aug 31	15.662 ± 0.054	15.616 ± 0.054	...	...	15.349 ± 0.054
1990 Sep 11	15.655 ± 0.007	15.653 ± 0.012	...	...	15.371 ± 0.008
1990 Sep 12	15.661 ± 0.010	15.653 ± 0.015	...	...	15.335 ± 0.009
1990 Sep 13	15.668 ± 0.019	15.661 ± 0.011	...	...	15.398 ± 0.015
1990 Sep 15	15.644 ± 0.005	15.651 ± 0.054	...	...	15.367 ± 0.037
1990 Sep 21	15.703 ± 0.011	15.681 ± 0.020	...	...	15.384 ± 0.011
1990 Sep 22	15.679 ± 0.006	15.690 ± 0.007	...	...	15.380 ± 0.026
1990 Sep 29	...	15.677 ± 0.028	...	...	15.354 ± 0.015
1990 Oct 12	15.741 ± 0.014	15.768 ± 0.054	...	...	15.430 ± 0.054
1990 Oct 16	...	15.715 ± 0.021	...	...	15.431 ± 0.048
1990 Oct 17	15.706 ± 0.014	15.692 ± 0.017	...	...	15.395 ± 0.026
1990 Oct 29	15.755 ± 0.054	15.705 ± 0.054	...	...	15.432 ± 0.054
1990 Nov 11.....	...	15.700 ± 0.009	...	...	...
1991 Feb 20	...	15.690 ± 0.038	...	...	...
1991 Feb 21	15.627 ± 0.011	...	...	...	...
1991 Sep 03	15.849 ± 0.029	15.823 ± 0.006	...	...	...
1991 Sep 05	15.846 ± 0.010	15.828 ± 0.021	...	...	...
		Capilla Peak Observatory (New Mexico)			
1990 Sep 21	...	...	15.44 ± 0.04	...	14.45 ± 0.08
1990 Sep 28	15.99 ± 0.05	...	15.62 ± 0.04	15.20 ± 0.06	14.49 ± 0.09
1990 Oct 13	15.85 ± 0.05	...	15.54 ± 0.04	15.27 ± 0.05	14.52 ± 0.08
		Landessternwarte Heidelberg			
1990 Sep 13	...	...	...	15.139 ± 0.018	...
1990 Sep 13	...	...	...	15.173 ± 0.018	...
1990 Sep 14	...	...	...	15.187 ± 0.018	...
1990 Sep 16	...	...	...	15.192 ± 0.018	...
1990 Sep 16	...	...	...	15.205 ± 0.019	...
1990 Sep 28	...	...	...	15.200 ± 0.019	...
1990 Oct 03	...	...	...	15.218 ± 0.019	...
1990 Oct 08	...	...	...	15.226 ± 0.019	...
1990 Oct 09	...	...	...	15.205 ± 0.019	...
1990 Oct 10	...	...	...	15.202 ± 0.019	...
1990 Oct 22	...	...	...	15.261 ± 0.020	...
1990 Oct 23	...	...	...	15.262 ± 0.020	...
1990 Dec 05	...	...	...	15.247 ± 0.019	...
1990 Dec 06	...	...	...	15.222 ± 0.019	...
1990 Dec 07	...	...	...	15.193 ± 0.018	...

m Shane telescope using the same filters. Eight of these nights were photometric. The 3 m has a smaller field of view so there were only two–three comparison stars in common with the 1 m field. The 1 m and 3 m frames were combined into one data set for input into the computer code which performed the relative photometry calculations. Any frame which had only one good comparison star was arbitrarily given an error bar of 5%, about twice the average observed error. The observations were referenced to spectrophotometric standard stars in Oke (1974), Oke & Gunn (1983), and Stone (1977). The resulting light curves are shown in Figure 1.

The Capilla Peak Observatory uses a 1.05 m telescope equipped with a CCD. Broadband photometry was obtained with the *B*, *V*, *R*, and *I* Johnson-Kron-Cousins filters. Absolute calibration is based on the Hayes & Latham (1975) calibration of Vega using the effective wavelengths for the filters given by Landolt (1983).

Photometry at ~6200 Å was also performed between 1990 September 13 and December 7 with the 70 cm telescope at the Landessternwarte Heidelberg equipped with a CCD (GEC, 576 × 386 pixel, 0″.85 pixel^{-1}) with a Johnson *R* filter (Table 4, bottom section). The integration time for each exposure was ~1200 s. Due to the observing conditions, no absolute calibration could be performed. The reduction included bias subtraction and flat fielding via "sky flats." The fluxes of the source and of several comparison stars were measured using the Daophot package. By computing the normalized ratios of the target fluxes versus the comparison stars the light curve was derived (Fig. 1*e*). The error bars correspond to 1 σ uncertainties. The fluxes were then calibrated according to the Capilla Peak *R* photometry, on the basis of two simultaneous observations (September 28) and the calibrated magnitudes are given in Table 4.

The photometric data in the different bands and the spectrophotometry at the corresponding effective wavelengths are generally consistent to within ~10%–15%.

Table 5 shows a comparison of the mean photometry taken at three different telescopes. Agreement is good ($\lesssim$10%) in all

TABLE 5

X-RAY, UV, AND OPTICAL PROPERTIES

Band	λ^a (Å)	Instrument	$\langle F \rangle$ (mJy)	$\sigma_F{}^b$	χ^2
X.....	12.4	*ROSAT* + PSPC	0.85×10^{-3}	0.199	1.33
UV.....	1600	*IUE* + SWP	0.75	0.100	11.7
B'	4250	CCD[c] + Johnson	1.90	0.065	47.6
B.....	4400	CCD[d] + JKC	1.94	...	...
g'.....	4900	CCD[c] + Gunn	1.92	0.050	38.0
V.....	5500	CCD[d] + JKC	2.23	...	...
R'	6200	CCD[c] + Johnson	1.00[f]	0.030	4.02
R.....	6800	CCD[d] + JKC	2.37	...	...
I'	8000	CCD[c] + KC	2.56	0.029	4.70
I.....	8250	CCD[d] + JKC	3.87	...	...

[a] Central wavelength.

[b] Variability index calculated (only for $N > 3$) as in Edelson 1992:

$$\sigma_F = \frac{1}{\langle F \rangle}\left[\frac{1}{N-1}\sum_{i=1}^{N}(F_i - \langle F \rangle)^2\right]^{1/2}$$

[c] On the Lick Observatory 1 m and 3 m telescopes.

[d] On the Capilla Peak Observatory 1.05 m telescope.

[e] On the Landessternwarte Heidelberg 70 cm telescope.

[f] Relative normalization.

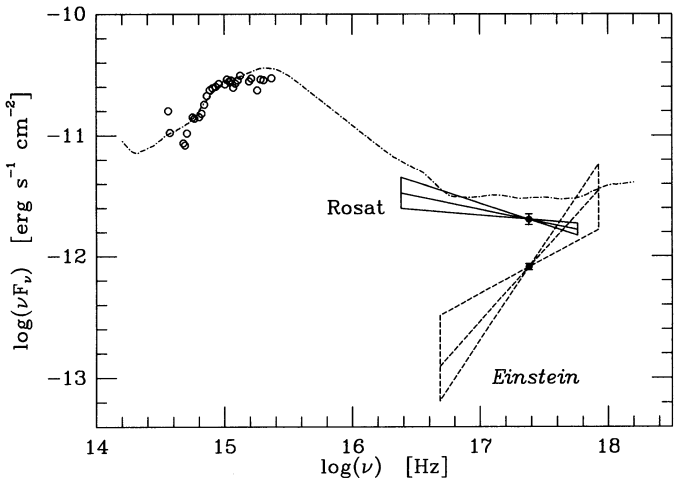

FIG. 6.—Overall spectral energy distribution. The open dots represent the *I*-band fluxes (Capilla Peak, 1990 October 13; and Lick Observatory, October 16), the optical (MMT, 1990 October 15) and the UV (*IUE* with SWP and LWP, October 14) data. The solid lines correspond to the best fit and 1 σ confidence range of the average *ROSAT* spectrum. The dashed lines are the fit and 1 σ confidence range of the 1979 *Einstein* observation. The dotted-dashed curve represents the median radio-quiet quasar spectral energy distribution as from Elvis et al. (1994).

cases except the *I* band, which shows a 40% discrepancy. This discrepancy has not been resolved and we thus adopt a larger error for the *I* points ($\pm 20\%$).

The optical-UV light curves indicate some dimming of the source in the first part of the observation, most prominently in the *B* band. A brightening at MJD = 8300 is apparent in *B* and UV light curves. Comparable X-ray variability may be masked by the large uncertainties.

4. DISCUSSION

The light curves at the different frequencies show some variability of the source during our monitoring. In Table 5 we give the intrinsic variability parameter for the various bands. The variability increases regularly with increasing frequency. There is a suggestion of a correlation between the various bands, but unfortunately the UV and optical points are too scarce and unevenly spaced to look for lags between the various light curves. Moreover, the uncertainties on the X-ray flux are rather large, which prevents a reliable determination of lags (see, e.g., Edelson et al. 1995, for a discussion on these points).

Our observations allow us to construct the simultaneous composite continuum spectrum from the *I* band to the X-rays, which is given in Figure 6. Both *I* fluxes obtained by us are reported. UV and optical continuum fluxes have been corrected for the extinction with $A_V = 0.3$, based on the Galactic column density $N_H = 5.0 \times 10^{20}$ (Elvis et al. 1989), a gas-to-dust ratio $N_H/E_{B-V} = 5.2 \times 10^{21}$ cm^{-2} mag^{-1} (Shull & Van Steenberg 1985) and $R = 3.1$ (Rieke & Lebofsky 1985) for the ratio of total to selective extinction. The dereddening follows Seaton (1979). The UV-optical data correspond to 1990 October 14 and 15, respectively, while for the X-rays we report the power-law fit of the averaged *ROSAT* spectrum. For comparison, the *Einstein* spectrum is also reported.

The median radio-quiet quasar spectral energy distribution proposed by Elvis et al. (1994) has been superposed on the present data, after suitable rescaling to the redshift of the object, and it reproduces satisfactorily the overall spectrum (see Fig. 6). In the *I* band there is a spectral rise, which is characteristic of the class. McDowell, Elvis, & Wilkes (1992), on the basis of *IRAS* observations, noted that the source is relatively infrared weak above ~ 10 μm. We have no new infrared data to confirm this weakness. The 1200–4300 Å range is well fitted by a power law of energy index $\alpha_\nu \simeq 0.9$ ($F_\nu \propto \nu^{-\alpha_\nu}$), which is typical for radio-quiet quasars (see, for PG quasars, Pian & Treves 1993).

In Figure 6 it can be seen that an extrapolation of the *ROSAT* X-ray spectrum underestimates the UV flux by a factor of ~ 5. The interpolation from 1500 Å to 1 keV yields a slope $\alpha_\nu = 1.5$. The fact that the UV data lie above the extrapolation of the X-rays suggests the presence of a soft X-ray excess (Walter & Fink 1993), which is not unusual for this class of objects. However, evidence for a soft component within the X-ray data is weak, since the best-fit column density is close to the Galactic one, and the single power-law fit is acceptable ($\chi^2 \simeq 0.9$). On the other hand, the soft component may ease the problem of matching the UV to the X-rays. Taking a temperature of 21 eV (see Table 1) corresponding to the blackbody + power law best fitted to the *ROSAT* spectrum, one can account for 10% of the 1200 Å flux. The linear dimension of the black body emitting region is 10^{12}–10^{13} cm, a value somewhat lower than those considered for thermal emission in quasars (Malkan & Sargent 1982). If the blackbody temperature were lower, one could account for a larger fraction of the UV, and at the same time increase the size of the region responsible for thermal emission. However, the fraction of the total blackbody flux which enters in the *ROSAT* range (0.1–2.4 keV), which is 50% for $T = 21$ eV, would become substantially smaller and the hypothesis of the thermal component would appear even more ad hoc. The same considerations prevent us from searching for a fit with a more complex thermal component as, e.g., an accretion disk spectrum.

The *ROSAT* X-ray slope is rather typical of radio-quiet quasars. The sample of 21 radio-quiet quasars observed with *Einstein* (0.2–3.5 keV) gives in fact $\langle \Gamma \rangle = 2.0 \pm 0.1$ (Shastri et al. 1993), while a sample of 53 radio-quiet quasars observed with *ROSAT* yielded $\langle \Gamma \rangle = 2.54 \pm 0.04$ (Schartel, Walter, &

Fink 1994), indicating that within this sample Kaz 102 is among those with harder spectra.

The most important result of our observations is that the *ROSAT* spectrum is substantially softer than that obtained from the *Einstein* data. It seems hard to ascribe such a large difference to the different energy ranges of the two instruments which do not overlap completely. Some systematic differences between indices measured with the two instruments are indeed reported by various authors. However, these are around $\Delta\Gamma \simeq 0.6$–0.7 (Fiore et al. 1994; Schartel et al. 1994). Brunner et al. (1994) find for a sample of radio–selected quasars that the *Einstein* IPC spectral slopes are consistent with the *ROSAT* ones at 90% confidence. The difference $\Delta\Gamma = 1.1$ found by us (see § 2.2) with 5 σ confidence appears to be significant. Therefore we are led to consider that the variation is real. The spectrum remains steep for the entire duration of the *ROSAT* observation and its slope is consistent with the average value of radio-quiet quasars, thus probably a somewhat unusual state was detected by *Einstein*, which leads the object at the extreme of the hardness distribution of quasars and makes it an interesting target for observation at higher energies. The fact that in the low state the spectrum is very flat and in the higher state a thermal component may show up, indicate that the energy distribution is rather complicated and that the power-law fits, even if formally acceptable are most probably inadequate.

The flux variations in the X-rays, between the *Einstein* and *ROSAT* observations, and the UV do not appear exceptional for a quasar if compared with the archives (Cutri et al. 1985; Maccacaro, Garilli, & Mereghetti 1987; O'Brien, Gondhalekar, & Wilson 1988; Kinney et al. 1991). Based on the spectral variability observed with *EXOSAT* (0.1–8 keV) in a sample of bright active galactic nuclei (mostly Seyfert galaxies; Grandi et al. 1992), the variability is not unprecedented.

We thank J. McDowell and M. Elvis for critical reading of the manuscript. S. J. W. and J. H. acknowledge partial support by the DFG through SFB 328. The *ROSAT* mission is supported by the Ministerium für Forschung und Technologie (BMFT), Germany, and by the Max-Planck-Gesellschaft.

REFERENCES

Bohlin, R., Harris, A. W., Holm, A. V., & Gry, C. 1990, ApJS, 73, 413
Brinkmann, W., & Trümper, J. 1992, MPE Rep., No. 235
Brunner, H., Lamer, G., Worrall, D. M., & Staubert, R. 1994, A&A, 287, 436
Cassatella, A., Lloyd, C., & Gonzalez-Riestra, R. 1988, *IUE* ESA Newsletter, 31, 13
Cutri, R. M., Wisniewski, W. Z., Rieke, G. H., & Lebofsky, M. J. 1985, ApJ, 296, 423
Edelson, R. A. 1992, ApJ, 401, 516
Edelson, R. A., et al. 1995, ApJ, 438, 120
Elvis, M., et al. 1994, ApJS, 95, 1
Elvis, M., Lockman, F. J., & Wilkes, B. J. 1989, AJ, 97, 777
Falomo, R., Treves, A., Chiappetti, L., Maraschi, L., Pian, E., & Tanzi, E. G. 1993, ApJ, 402, 532
Fiore, F., Elvis, M., McDowell, J. C., Siemiginowska, A., & Wilkes, B. J. 1994, ApJ, 431, 515
Grandi, P., Tagliaferri, G., Giommi, P., Barr, P., & Palumbo, G. 1992, ApJS, 82, 93
Hayes, D. S., & Latham, D. W. 1975, ApJ, 197, 593
Kinney, A. L., Bohlin, R. C., Blades, J. C., & York, D. G. 1991, ApJS, 75, 645
Landolt, A. 1983, AJ, 88, 439
Maccacaro, T., Garilli, B., & Mereghetti, S. 1987, AJ, 93, 1484
Malkan, M. A., & Sargent, W. L. W. 1982, ApJ, 254, 22
McDowell, J. C., Elvis, M., & Wilkes, B. J. 1992, in AIP Conf. Proc. 254, Testing the AGN Paradigm, ed. S. Holt, S. G. Neff, & C. M. Urry (New York: AIP), 532
Morrison, R., & McCammon, D. 1983, ApJ, 270, 119
Netzer, H. 1990, in Proc Saas-Fee Advanced Course 20, Active Galactic Nuclei, ed. T. J.-L. Courvoisier & M. Mayor (Berlin: Springer), 62
O'Brien, P. T., Gondhalekar, P. M., & Wilson, R. 1988, MNRAS, 233, 845
Oke, J. B. 1974, ApJS, 27, 21
Oke, J. B., & Gunn, J. E. 1983, ApJ, 266, 713
Pian, E., & Treves, A. 1993, ApJ, 416, 130
Rieke, G. H., & Lebofsky, M. J. 1985, ApJ, 288, 618
Schaeidt, S. 1994, Ph.D. thesis, Ludwig-Maximilian Universität, München
Schartel, N., Walter, R., & Fink, H. H. 1994, A&A, submitted
Seaton, M. J. 1979, MNRAS, 187, 73p
Shastri, P., Wilkes, B. J., Elvis, M., & McDowell, J. C. 1993, ApJ, 410, 29
Shull, J. M., & Van Steenberg, M. E. 1985, ApJ, 294, 599
Snowden, S. L., McCammon, D., Burrows, D. N., & Mendenhall, J. A. 1994, ApJ, 424, 714
Stone, R. P. S. 1977, ApJ, 218, 767
Treves, A., et al. 1992, MPE Rep., No. 235, p. 175
Urry, C. M., & Reichert, G. 1988, *IUE* NASA Newsletter, 34, 96
Walter, R., & Fink, H. H. 1993, A&A, 274, 105
Wilkes, B. J., & Elvis, M. 1987, ApJ, 323, 243